Acta Cryst. (1959). **12**, 976

Quantitative Treatment of Multiple Scattering Effect in Continuous Electron Diffraction Curves

BY J. GJØNNES

Central Institute for Industrial Research, Oslo, Norway

(*Received* 1 *April* 1959)

The theory of noncoherent multiple scattering is reviewed and calculation procedures are derived which permit the conversion of an experimental intensity distribution given in a limited angular region and corresponding to a thickness t into (*a*) the intensity distribution corresponding to a thickness nt, (*b*) the single scattering cross section. The background and oscillating terms are treated separately. The methods are applied to diffractograms obtained from evaporated carbon films in the thickness range 100–600 Å using an accelerating voltage of 36 kV.

1. Introduction

Effects of multiple scattering in electron-diffraction experiments have been considered by several authors; in single crystal patterns by Cowley, Rees & Spink (1951) and in powder patterns by Ellis (1952). An estimate of the magnitude of multiple scattering in gas investigations has been made by Karle & Karle (1950).

Little effort seems to have been made, however, to utilize the theory of multiple scattering of fast particles as derived by Goudsmit & Saunderson (1940), Moliere (1948) and Bethe (1953) in the investigation of such effects, and it is the purpose of this paper to demonstrate how this may be done in the interpretation of the continuous intensity curves obtained in transmission diffraction. The investigation has been carried out with special reference to amorphous carbon films prepared by evaporation but the methods should be applicable to scattering from a gas jet or a polycrystalline film as well.

It should be mentioned that measurements of continuous electron-diffraction curves are carried out in a limited angular region, usually $s \sim 1$ Å^{-1} to $s \sim 40$–60 Å^{-1} where $s = 4\pi \sin\theta/\lambda$, λ the wavelength and 2θ the scattering angle. The observed intensity is as a rule split into two parts: a smooth background term corresponding to the structure-independent coherent and incoherent scattering and an oscillating or structure dependent term (I_M) (see for example Hassel & Viervoll, 1947). Whereas excellent agreement has been obtained between theoretical and experimental I_M-curves in gas investigations, experimental and theoretical background are often discrepant.

The main goal of this investigation has been to establish computational methods suitable to treatment of the limited angular region comprised by ordinary diffraction experiments and the oscillating term of the intensity has been subject to special considerations. The multiple scattering effects to be considered are: (i) The substantial variation in background shape with thickness, (ii) the concurrent decrease and smoothing out of the oscillating term, (iii) thickness-dependent details in the oscillating term.

2. Theory of multiple scattering

Let the distribution, normalized over the unit sphere, of electron scattered from a sheet of thickness Δt be $\sigma_1(\mathbf{k}-\mathbf{k}_0)$ where $\mathbf{k}$ and $\mathbf{k}_0$ are wave vectors in the direction of the scattered and undeviated beam respectively. The total distribution of a beam of electrons after traversing one such sheet is then

$$I_1(\mathbf{k}-\mathbf{k}_0) = (1-\mathscr{H})\delta(\mathbf{k}-\mathbf{k}_0) + \mathscr{H}\sigma_1(\mathbf{k}-\mathbf{k}_0) \quad (1)$$

where $\mathscr{H}$ is the scattered fraction of the electrons and δ is a 2-dimensional Dirac δ-function. After traversing two sheets, the angular distribution will be given by a convolution integral taken over the unit sphere:

$$I_2(\mathbf{k}-\mathbf{k}_0) = \int I_1(\mathbf{k}-\mathbf{k}_1) I_1(\mathbf{k}_1-\mathbf{k}_0)\, dw_1$$

if we assume equal path lengths in the two sheets and that there is no structural coherence* between the sheets. The extension to n sheets is obvious and can be given in the form

$$\begin{aligned} I_n(\mathbf{k}-\mathbf{k}_0) &= (1-\mathscr{H})^n \delta(\mathbf{k}-\mathbf{k}_0) \\ &\quad + n(1-\mathscr{H})^{n-1}\mathscr{H}\sigma_1(\mathbf{k}-\mathbf{k}_0) \\ &\quad + \tfrac{1}{2}n(n-1)(1-\mathscr{H})^{n-2}\mathscr{H}^2\sigma_2(\mathbf{k}-\mathbf{k}_0)t \ldots \end{aligned} \quad (2)$$

where

$$\sigma_m(\mathbf{k}-\mathbf{k}_0) = \int\ldots\int \sigma_1(\mathbf{k}-\mathbf{k}_1)\ldots\sigma_1(\mathbf{k}_{m-1}-\mathbf{k}_0)\, dw_1 \ldots dw_{m-1} \quad (2a)$$

* The implications of the latter assumption and the relationship of this multiple scattering theory to the wave optical approach of Cowley & Moodie (1957) is indicated in an appendix.

may be defined as mth order scattering with σ_1 as the fundamental scattering cross section.

The convolution integrals (2a) can be evaluated by expanding σ_1 in spherical harmonics. We shall assume cylindrical symmetry about the undeviated beam, such that the series will include only Legendre functions of the scattering angle 2θ:

$$\sigma_1 = \Sigma(2l+1) f_l P_l(\cos 2\theta)/4\pi .$$

Introducing this expansion in (2a) we obtain by use of well-known integrals (see for example Morse & Feshbach, 1953, p. 1327)

$$\sigma_m = \Sigma(2l+1)(f_l)^m P_l(\cos 2\theta)/4\pi \qquad (3)$$

and

$$F_{ln} = [(1-\mathscr{H}) + \mathscr{H} f_l]^n \qquad (4)$$

where F_{ln} are the Legendre coefficients of I_n. If we now can let $\Delta t \to 0$, the Legendre coefficient of the distribution of emerging electrons, including the undeviated beam, will be

$$F_l = \exp[-\mu t(1-f_{0l})] . \qquad (5)$$

Here μ is the extinction coefficient, t total thickness and f_{0l} the coefficients of 1. order scattering. This equation was first derived by Goudsmit & Saunderson (1940).

In the following we shall restrict ourselves to the case of small angles where the unit sphere can be replaced by its tangent plane. The Legendre-expansions (3) are then replaced by the Fourier–Bessel expansions

$$\sigma_m(s) = \int_0^\infty l' J_0(l's) f^m(l') dl' \qquad (6)$$

where we for convenience have replaced the scattering angle 2θ by s as the variable in intensity space assuming $\theta \approx \sin\theta$. A corresponding change (l to l') is made in coefficient space and in the normalization. Equations (4) and (5) still apply and may in principle be used for the purposes outlined in the introduction. The measured intensity distribution is expanded as a Fourier–Bessel integral by taking the (Hankel-)transform

$$f(l') = \int s\sigma(s) J_0(sl') ds .$$

Using equation (4) or (5), the coefficient f for an arbitrary thickness may be found and by means of a new Hankel transform the corresponding intensity distribution is obtained.

The theory above rests on the following assumptions: (i) Energy loss can be neglected, (ii) path differences can be neglected, (iii) the unit sphere can be approximated by its tangent plane.

According to Marton (1956) the energy losses suffered by the electrons are only a few electron volts and are thus quite insignificant. The influence of path differences has been considered by Wang & Guth (1951), and can be shown to be negligible. The implications of (iii) can be considered by introducing the more accurate approximation (see Bethe (1953))

$$P_l(\cos u) \approx (u/\sin u)^{\frac{1}{2}} J_0[(l+\tfrac{1}{2})u]$$

in the Legendre expansion. The resulting corrections to our calculations turn out to be of the order 1% at the highest angle ($s = 20$ Å^{-1}).

3. Application to electron-diffraction curves

Based on the general theory outlined above, we shall now describe computational procedures for two purposes: (*a*) converting the measured intensity distribution obtained from a film of given thickness into an intensity curve corresponding to a multiple of this thickness, in order that relevant comparison can be made between diffractograms obtained from films of different thickness; (*b*) reduction of a measured intensity distribution to 1. order scattering cross section.

The calculations of type (*a*) turn out to be by far the simplest and may proceed as follows: In the observation region, s_A to s_B, the measured intensity is expressed as a sum of an analytical (background) expression σ_B, with known Fourier–Bessel coefficient and a remainder term, σ_R, including molecular scattering. Outside the region s_A to s_B, the intensity distribution is approximated by σ_B. A particularly suitable form of σ_B is a sum of expressions $p(p^2+s^2)^{-3/2}$ with the coefficient $\exp(-pl')$ (see for example Morse & Feshbach, 1953, p. 1324). It is seen that the convolution in intensity space of two such expressions with parameters p_1 and p_2 results in a similar expression with the parameter p_1+p_2. The necessary convolution integrals (2a) for computation of higher-order scattering terms are then split into background and oscillating terms:

$$\sigma_1 * \sigma_1 = \sigma_B * \sigma_B + 2\sigma_B * \sigma_R + \sigma_R * \sigma_R \quad \text{etc.}$$

where $*$ denotes the convolution. The first one, which is a pure background term, is evaluated analytically as indicated above; for the last two terms we must resort to numerical integrations via the coefficient of σ_R.

The calculations of type (*b*) are not as easy, as the expression for the 1. order Fourier–Bessel coefficient takes the form

$$f_0(l') = 1 + \ln[\exp(-\mu t) + (1-\exp(-\mu t))f]/\mu t \qquad (7)$$

where f is the coefficient of $\sigma_B + \sigma_R$. A separation in background and oscillating terms is obtained by expanding as a power series in the coefficient of σ_R, but we cannot expect to find an analytical expression with a Fourier–Bessel coefficient with the form of the first term of this series, and have to rely on numerical integration for this term too.

The numerical integrations were in this investigation performed using a punched-card file for the Bessel

function J_0. The cards have been prepared for arguments 0–100 at intervals 0·02 and permit integer values -255 to $+255$ of the operand. The term σ_R should, therefore, satisfy the two requirements:

The coefficient should be negligible above

$$l'_{\text{max.}} \approx 100/s_B ,$$

and the amplitude of σ_R should not decrease by a factor comparable to 255 through the region (s_A to s_B). The first requirement is essential in transformation from coefficient to intensity space, and to meet this one when treating the background term in (*b*) we have to introduce analytical fits at high values of l'.

It remains to discuss the implications of extrapolating the measured intensity curve beyond the observation range by the expression σ_B. Consider the extrapolation towards greater angle first. Due to the steep decrease of σ with angle, a negligible fraction of the double scattering processes (s_1, s_2) contributing to the intensity at a given angle s will include single scattering through angles appreciably greater than s, and similarly for higher order scattering. The computed cross sections in the region s_A to s_B will thus be quite insensitive to the extrapolation towards greater angle, except at angles just below s_B. The error introduced by the extrapolation towards smaller angle can to some degree be compensated for by taking the remaining intensity as part of the undeviated beam. In double scattering this amounts to approximating part of the scattering processes (s_1, s_2) by single scattering through s_2 when $s_1 < s_A$. The error resulting from this approximation will largely be confined to angles just above s_A, but the parameter $\mathscr{H}$ of equation (2) must be replaced by $\alpha\mathscr{H}$ where α is the fraction of scattered electrons included in the distribution $\sigma_B + \sigma_R$.

4. Experimental

Carbon films in the thickness range 100–600 Å as measured in a multiple-beam interferometer were prepared by evaporation. Electron diffractograms were obtained by the diffraction apparatus at the University of Oslo using an accelerating voltage of approximately 36 kV. and a rotating s^3-sector. The distance between diffraction point and photographic plate was approximately 49 cm., and the intensity data covered the s-region 1·5–20 Å^{-1}. The photometer curves were corrected in the standard way for the sector function, non-linear blackening and oblique incidence. Corrected intensity curves multiplied by s^4 are shown (full-line) in Fig. 1 for 100, 325 and 600 Å thickness.

A number of diffractograms from a 100 Å-film were also taken without a sector to obtain intensity data in the region $s = 0{\cdot}2$–$1{\cdot}5$. The electron transmission through films of different thicknesses was measured by inserting a high-resistance voltmeter between the beam stop and ground terminal giving these mean values:

Thickness	110	170	350	450	600 Å
I/I_0	0·6	0·45	0·20	0·15	0·15

The 450Å film displayed somewhat greater variations than the others.

5. Calculations

Starting with the 100 Å-intensity curve in the region 1·5–20 Å^{-1} 300 and 600 Å intensity curves were calculated by the procedure (*a*) of sec. 3 using the approximation

$$\sigma_{100} = A_1 2(2^2 + s^2)^{-3/2} + A_2 10(10^2 + s^2)^{-3/2} + \sigma_R \quad (9)$$

where $A_1 = 1{\cdot}073$, $A_2 = -0{\cdot}073$, and σ_R is confined to the s-range 1·5–20 Å^{-1}. Calculations were performed for $\alpha\mathscr{H} = 0{\cdot}2$ and 0·3 at intervals $\Delta s = 0{\cdot}5$ for the background and $\Delta s = 0{\cdot}25$ for the oscillating terms. The calculated 300 and 600 Å intensity curves multiplied by s^4 are shown by the broken and dotted lines in Fig. 1.

To obtain an estimate of the parameter α, the ex-

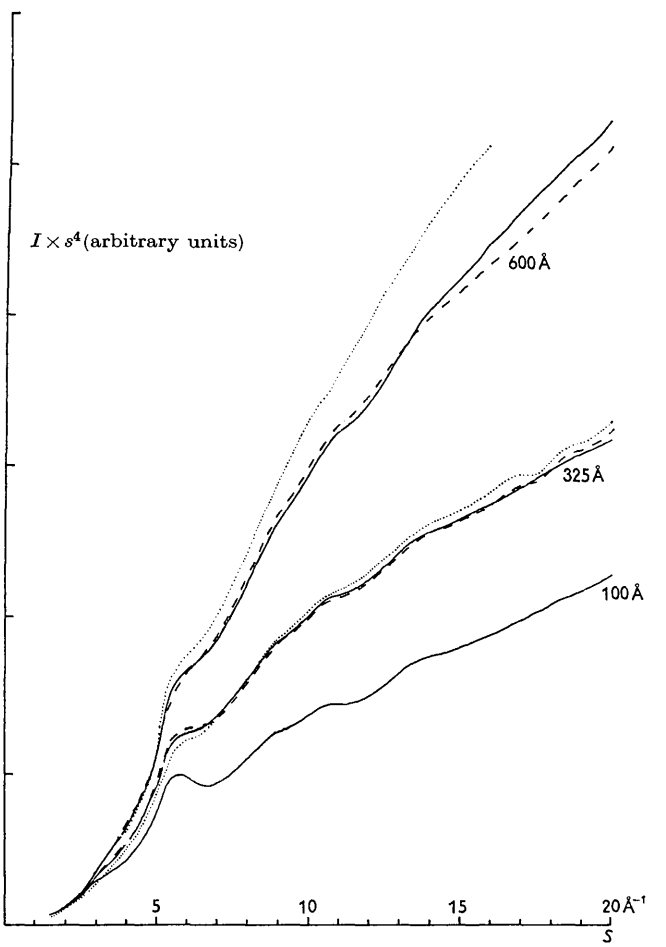

Fig. 1. Full-line: Experimental intensity curves multiplied by s^4 for 100, 325 and 600 Å. Broken: Calculated intensity curves (method *a*) for 300 and 600 Å, $\alpha\mathscr{H} = 0{\cdot}2$. Dotted curves: Calculated intensity for 300 and 600 Å, $\alpha\mathscr{H} = 0{\cdot}3$.

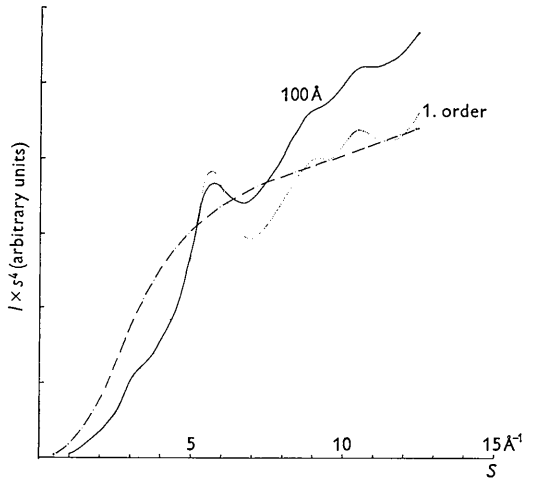

Fig. 2. Full-line: Experimental intensity curve for 100 Å. Dotted: Calculated 1. order scattering. Dash-dotted: Theoretical background.

pression (9) was compared with the intensity curve below $s=1{\cdot}5$ Å^{-1} obtained without the sector. α was found to be about 0·75 so that the calculations above correspond to $\mathscr{H}$-values 0·27 and 0·4 for a 100 Å film.

Starting with the 100 Å intensity curve

$$\sigma_{100}=B\exp(-7s)+A_1'2(2^2+s^2)^{-3/2}+A_2'10(10^2+s^2)^{-3/2}+\sigma_R'$$

where $B=8{\cdot}46$, $A_1'=0{\cdot}829$, $A_2'=-0{\cdot}057$ and σ_R' is confined to the s-region 0·2–20 Å^{-1}, 1. order intensity up to $s=18$ was calculated from a series expansion of (8) to the second power in f_R using the $\mathscr{H}$-value 0·4. As explained in sec. 3 a combination of analytical fits and numerical integration had to be used in the calculation of the background term. Due to the steep decrease of background with s and the limitations of the punched card file, the background term is very inaccurate at high angle. It is believed, however, that the calculations are fairly accurate for the background below $s=7$ and for the oscillating terms below $s=15$. Owing to the extensive computational labor and the fact that greatest interest usually is taken in the oscillating term, the calculations were not pursued further. A comparison between the computed 1. order scattering (dotted), 100 Å intensity (full-line) and theoretical background, $(Z-F)^2+S$, is given in Fig. 2.

The atom form factor F corresponding to $Z=6$ was taken from Berghuis *et al.* (1955), and the incoherent scattering intensity, S, from Milberg & Brailsford (1958).

Molecular scattering intensities, I_M, corresponding to the calculated and experimental intensity curves were obtained by subtracting smooth background curves and are shown in Fig. 3 after multiplication with $s/(Z-F)^2$ and division by the corresponding background value at $s=8$.

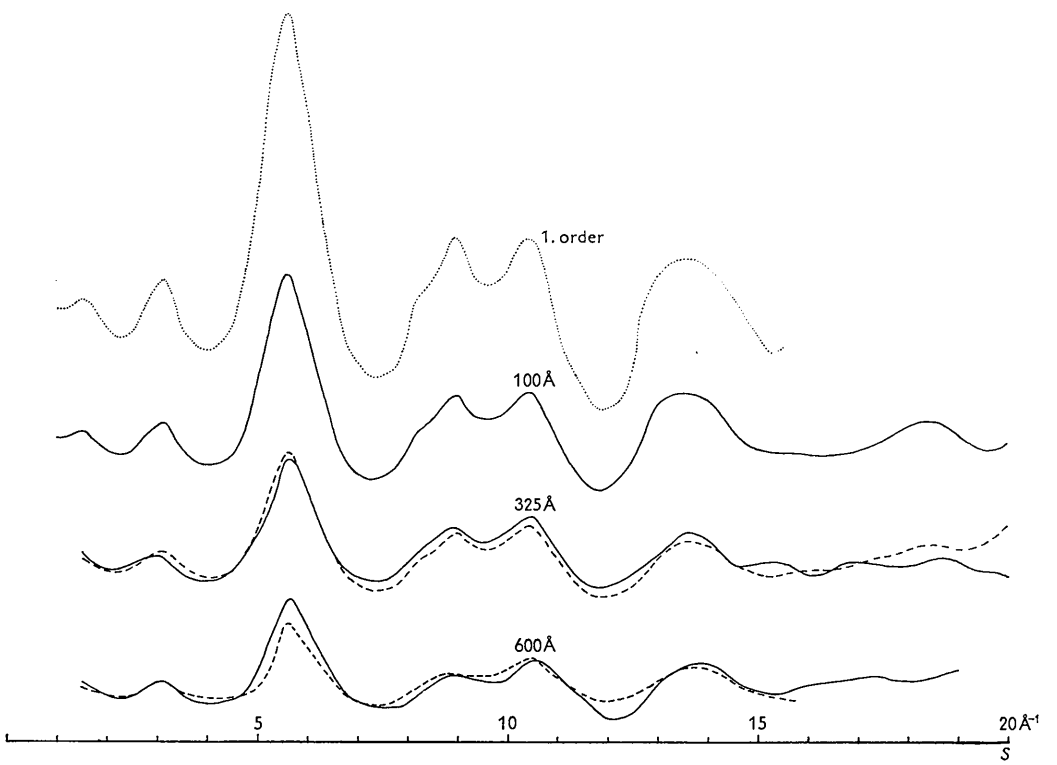

Fig. 3. Full-line: Experimental molecular scattering curves, 100, 300 and 600 Å. Broken: Molecular scattering curves obtained from calculated intensity curves, $\alpha\mathscr{H}=0{\cdot}2$. Dotted: Molecular scattering from the calculated 1. order scattering.

6. Conclusions

The preceding calculations of type (*a*) show that the thickness-dependent variations in the diffractograms of carbon films 100–600 Å thick can, within experimental error, be ascribed to non-coherent multiple scattering, and it may be inferred that the diffractograms indicate no structural variations with thickness. The variations in the oscillating term are rather small, but a marked effect at $s \sim 10$ is clearly seen in Fig. 3.

The calculations may be carried out without knowledge of the scattered intensity at the smallest angles, if the scattered fraction of electrons is taken as an *adjustable* parameter. The attempt to connect this adjusted value $\alpha\mathscr{H}$ with the measured electron transmission did not quite succeed; the $\mathscr{H}$ value obtained from the transmission measurement being 0·4, whereas the best fit, corrected for the intensity below $s=1{\cdot}5$ Å^{-1}, gives 0·27. The reason for this discrepancy is not understood, but it should be pointed out that the intensity curve below $s=1{\cdot}5$ was obtained by overlapping a number of exposures and is very uncertain. The fact that the calculations account simultaneously for the variations in background and oscillating terms indicates, however, that they are essentially correct.

The calculation of 1. order scattering could not with the computational facilities at disposal, be made as accurate in the background term, and the failure to fit to the theoretical background should not be stressed, as this is the usual in gas investigations too. It seems likely, though, that a normalization to theoretical background using this calculated curve will be a considerable improvement from the direct use of the 100 Å intensity. The calculations of oscillating terms are expected to be as accurate as those of type (*a*).

A structural interpretation of the molecular scattering will be reported elsewhere.

APPENDIX

The non-coherent multiple scattering theory employed above may be derived from the scattering theory of Cowley & Moodie (1957) by giving the assumption of structural non-coherence an appropriate mathematical formulation as indicated below:

Consider a number of sheets perpendicular to the electron beam and with potential distributions $\varphi_j(\rho)$ where ρ is a vector in the plane of the sheets. From the general equations of Cowley & Moodie (1957) we obtain in the tangent-plane approximation, the angular distribution of the transmitted beam

$$I_A(\mathbf{s}) = \int \exp(i\mathbf{s}\rho') \int \exp\{i\tau[\Sigma\varphi_j(\rho) - \Sigma\varphi_k(\rho+\rho')]\} df\, df'$$

where $\mathbf{s}$ is the scattering vector and τ is a constant. The multiple-scattering theory applied to the Cowley–Moodie intensity from isolated sheets takes the form

$$I_B(\mathbf{s}) = \int \exp(i\mathbf{s}\rho') \prod_j \int \exp\{i\tau(\varphi_j(\rho) - \varphi_j(\rho+\rho'))\} df\, df' .$$

The assumption of non-coherence between the sheets may be formulated in a series of equations, of which we quote only two:

$$\sum_{j\neq k} \int \varphi_j(\rho)\varphi_k(\rho+\rho')\, df \quad \text{independent of } \rho'$$

$$\sum_{j\neq k} \frac{1}{A^2} \int \varphi_j^2(\rho)\, df \int \varphi_k^2(\rho)\, df = \sum_{j\neq k} \frac{1}{A} \int \varphi_j^2(\rho)\varphi_k^2(\rho+\rho')\, df$$

where A is the area of the integration region. Comparing the power series expansions in τ term by term, I_A and I_B is then found to be equal. A similar treatment can be made of the Born series.

I am indebted to Dr H. Viervoll for suggesting this problem and for several helpful discussions. The author also wishes to express his thanks to A. Almenningen for preparing the electron diffractograms and to Norsk Regnesentral for computional assistance. The Norwegian Council for Science and the Humanities is gratefully acknowledged for financial support.

References

Bethe, H. A. (1953). *Phys. Rev.* **89**, 1256.
Berghuis, J., Haanappel, IJ. M., Potters, M., Loopstra, B. O., MacGillavry, C. H. & Veenendaal, A. L. (1955). *Acta Cryst.* **8**, 478.
Cowley, J. M., Rees, A. L. G. & Spink, J. A. (1951). *Proc. Phys. Soc.* A, **64**, 609.
Cowley, J. M. & Moodie, A. F. (1957). *Acta Cryst.* **10**, 609.
Ellis, S. G. (1952). *Phys. Rev.* **87**, 970.
Goudsmit, S. A. & Saunderson, J. L. (1940). *Phys. Rev.* **57**, 24.
Hassel, O. & Viervoll, H. (1947). *Acta Chem.-Scand.* **1**, 149.
Karle, J. & Karle, I. L. (1950). *J. Chem. Phys.* **18**, 957.
Marton, L. (1956). *Rev. Mod. Phys.* **28**, 172.
Milberg, M. E. & Brailsford, A. D. (1958). *Acta Cryst.* **11**, 672.
Moliere, G. (1948). *Z. Naturforsch.* **3a**, 78.
Morse, P. M. & Feshbach, H. (1953). *Methods of Theoretical Physics.* New York: McGraw-Hill.
Wang, M. G. & Guth, E. (1951). *Phys. Rev.* **84**, 1092.